5A.3

SURFACE REFERENCE TECHNIQUE REQUIRED FOR A PRIMITIVE RETRIEVAL ALGORITHM OF GPM/DPR

Shinta Seto*[1)], Toshio Iguchi[2)], and Taikan Oki[1)]
1) Institute of Industrial Science, University of Tokyo, Tokyo, Japan
2) National Institute of Information and Communications Technology, Tokyo, Japan

1. INTRODUCTION

The core satellite of the Global Precipitation Measurement (GPM) mission will be launched in 2013 with Dual-frequency Precipitation Radar (DPR) on. DPR is the successor of the Precipitation Radar (PR) on the Tropical Rainfall Measuring Mission (TRMM) satellite. DPR consists of a Ku-band (13.6GHz) radar and a Ka-band (35.5GHz) radar, the former of which is similar to PR. DPR is expected to give more accurate estimates in rain drop size distribution (DSD) and rain rate by taking advantages of dual-frequency observations. Methods to retrieve DSD and rain rate from dual-frequency observations have been studied for more than 20 years. Echo power observed by a space-borne precipitation radar is converted to radar reflectively factor (Z_m) at some ranges and surface backscattering cross section (σ^0) at earth surface. The number of observations by DPR is ideally $2n + 2$, where n is the number of ranges. For simplicity, we assume ideally perfect conditions of observation so that many obstacles such as ground clutter can be ignored.

Meneghini et al. (1992; called ME92) developed a retrieval method for an airborne dual-frequency precipitation radar. ME92 assumed that DSD obeys a two-parameter gamma function and they retrieved $2n$ DSD parameters from $2n + 2$ observations. They applied a surface reference technique (SRT) to estimate path integrated attenuation (PIA) by comparing σ^0 at a target pixel and σ^0 at nearby no-rain pixels (reference pixels). In SRT, it is generally assumed that the surface conditions between a target pixel and the reference pixels are same in terms of σ^0, but this assumption is not guaranteed and the difference in surface conditions often causes biases in PIA. A SRT is applied in the standard algorithm of PR (Iguchi et al. 2009) and Seto and Iguchi (2007) found that rainfall-induced changes in surface conditions affect σ^0 and yield biases in PIA and rain rate estimates. Moreover, instantaneous rain rate estimates over land could be largely biased if the land surface type of a target pixel is drastically different from that of the reference pixels. In case of airborne observations, unstable attitude of an airborne could change σ^0 and cause bias in PIA and rain rate estimates (Mardiana et al. 2004; called MA04).

MA04 proposed a new retrieval method without SRT and tested it with air-borne dual-frequency observations. While PIA is estimated by means of SRT before the retrieval in ME92, PIA is assumed before the retrieval in MA04. After the retrieval, PIA can be calculated from the retrieved DSD and is compared with the assumed PIA. Until calculated and assumed PIAs are judged to be same, the assumed PIA is modified and the retrieval is iterated. The details of methods in ME92 and MA04 will be given in Section 3. MA04's method showed a good performance for the air-borne observations in their paper, but some following researches such as Rose and Chandrasekar (2005) and Liao and Meneghini (2005) claimed that MA04's method fails for relatively heavy rainfall cases. Adhikari et al. (2007) also showed cases of failure in MA04's method and proposed a modified method by using differential attenuation (DA) between the two frequencies. As DA can be estimated accurately only when rain rate is vertically constant or the Mie effect is negligible, the modified method can not be widely used.

As no methods without SRT are found to work for all cases, the necessity of SRT is strongly implied. This study examines the reason why MA04's method fails for heavier rainfall, confirms the necessity of SRT, proposes a new retrieval method, and discusses on the accuracy of SRT required to

* *Corresponding author address*: Shinta Seto, Institute of Industrial Science, University of Tokyo, 4-6-1, Komaba, Meguro-ku, Tokyo, Japan, 153-8505; e-mail: seto@iis.u-tokyo.ac.jp

retrieve surface rain rate within a certain error tolerance.

2. OBSERVATIONS BY DPR

2.1. Assumptions

DPR observes precipitation in nadir direction (with the incident angle of 0 degree) to obtain Z_m at n ranges and σ^0 at the surface (Fig. 1). The depth of each range is constant to be L [km]. Throughout this study, L is set as 0.25 km. Numbers 1 to n are assigned to ranges from the top to the bottom, then the height of precipitation can be given as $n \times L$. Rain drops are equally distributed in each range both vertically and horizontally, and the DSD follows a gamma distribution function as shown in Eq. (1).

$$N(D) = N_0 D^{\mu} \exp\left[-(3.67+\mu)D/D_0\right], \quad (1)$$

where D [mm] is drop size and N [mm^{-1} m^{-3}] is number density. N_0 [mm$^{-1-\mu}$ m^{-3}], D_0 [mm], and μ [-] are DSD parameters. In this study, μ is treated as a known parameter, and N_0 and D_0 are parameters to be estimated. Other particles than rain drops can be totally ignored.

2.2. Theory

Rain rate (denoted by R [mm h^{-1}]) can be calculated from the DSD parameters as Eq. (2).

$$R = C_R \int_{D=0}^{\infty} v(D) D^3 N(D) dD, \quad (2)$$

where C_R is a constant for unit conversion (=0.6$\pi \times 10^{-3}$) and $v(D)$ [m s^{-1}] is the falling velocity of rain drop and is dependent on D. According to Gunn and Kinzer (1949), we employ the following Eq. (3) to calculate $v(D)$.

$$v(D) = 4.854 \times D \times \exp(-0.195D). \quad (3)$$

Real (non-attenuated) radar reflectively factor (denoted by Z_e [mm6 m-3]) and attenuation coefficient (denoted by k [dB km^{-1}]) are given as Eqs. (4) and (5).

$$Z_e = C_Z \int_{D=0}^{\infty} \sigma_b(D) N(D) dD, \quad (4)$$

$$k = C_k \int_{D=0}^{\infty} \sigma_t(D) N(D) dD, \quad (5)$$

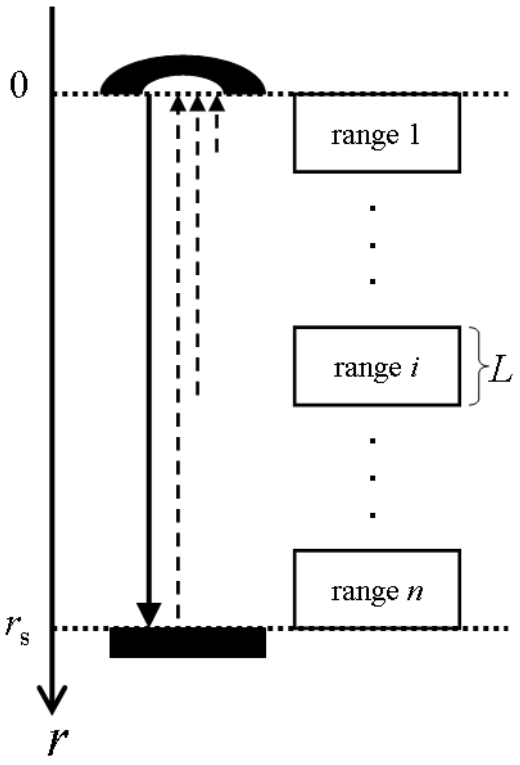

Fig. 1 A schematic figure of assumed DPR observation.

where $\sigma_b(D)$ [mm^2] and $\sigma_t(D)$ [mm^2] are backscattering cross section and total extinction cross section and the both are calculated from Mie theory. C_k is equal to $0.01 \times \log_{10}(e)$, and C_Z is given in Eq. (6).

$$C_Z = \frac{\lambda^4}{\pi^5} \left| \frac{n_w^2 + 2}{n_w^2 - 1} \right|^2, \quad (6)$$

where λ [cm] is the wavelength of microwave, n_w [-] is the refractivity index of water, which depends on the physical temperature of water (denoted by T [K]).

Measured (attenuated) radar reflectivity factor (denoted by Z_m [mm^6 m^{-3}]) at the distance of r [km] from the top of precipitation is calculated as Eq. (7).

$$Z_m(r) = Z_e(r) \exp\left(-0.2 \times \ln 10 \times \int_{s=0}^{r} k(s) ds \right), \quad (7)$$

where s is a dummy parameter of r. Equation (7) can be rewritten in dB unit as Eq. (8).

$$dBZ_m(r) = dBZ_e(r) - 2\int_{s=0}^{r} k(s) ds, \quad (8)$$

where dBX indicates $10\log_{10}(X)$ for any variable X. Given that r=r_s at the earth surface, PIA [dB] can be

written as Eq. (9).

$$\mathrm{PIA} = 2\int_{s=0}^{r_s} k(s)ds \qquad (9)$$

2.3. In discrete form

At a range, dBZ_e and k are determined only by parameters of the range, so they can be written as Eq. (10) and Eq. (11).

$$\mathrm{dB}Z_e(N_0,D_0)=10\log_{10}N_0+F(D_0), \qquad (10)$$

$$k(N_0,D_0)=N_0\times G(D_0), \qquad (11)$$

where F and G are functions of D_0 and the details are given as below.

$$F(D_0)=10\log_{10}\left\{C_Z\int_{D=0}^{\infty}\sigma_b(D)D^{\mu}\exp[-(3.67+\mu)D/D_0]dD\right\}, \qquad (12)$$

$$G(D_0)=C_k\int_{D=0}^{\infty}\sigma_t(D)D^{\mu}\exp[-(3.67+\mu)D/D_0]dD. \qquad (13)$$

On the other hand, Z_m at a range can not be determined by parameters of the range. When the range locates between $r=r_0-L/2$ and $r=r_0+L/2$ (Fig. 2), the average of Z_m (denoted by $[Z_m]$) at the range can be calculated as Eq. (14).

$$[Z_m]=\frac{1}{L}\int_{r_0-L/2}^{r_0+L/2}Z_m(r)dr=\frac{1}{L}\int_{r_0-L/2}^{r_0+L/2}Z_e(r)\exp\left(-0.2\times\ln 10\times\int_{s=0}^{r}k(s)ds\right)dr. \qquad (14)$$

As Z_e and k are constant within the range, Eq. (14) can be simplified as Eq. (15).

$$[Z_m]=Z_m(r_0)\frac{[\exp(cL/2)-\exp(-cL/2)]}{cL}, \qquad (15)$$

where c is equal to $0.2\times(\ln 10)\times k$. As c and L are positive, $[Z_m]$ is always larger than $Z_m(r_0)$. When c or L approaches to zero, $[Z_m]$ approaches to $Z_m(r_0)$. In other words, when the rainfall is weak enough or when the width of the range is thin enough, the attenuation from which the range suffers can be regarded to occur along the two-way path between the top of precipitation and the center of the range. This attenuation is indicated by dBA as shown in Fig. 2. Generally, the attenuation can be different from dBA, but it should be larger than dBA[-] and should be smaller than dBA[+], where dBA[-] (dBA[+]) are the attenuation along the two-way path between the top of precipitation and the top (bottom) of the range.

In many previous researches including ME92 and MA04, the attenuation is set as dBA[+], while the attenuation is set as dBA in some researches such as Kozu et al. (1991). No researches are found to set the attenuation as dBA[-]. To compare our results with those of ME92 and MA04, the attenuation is set as dBA[+] also in this study (except for section 6d), therefore dBZ_m is given as Eq. (16).

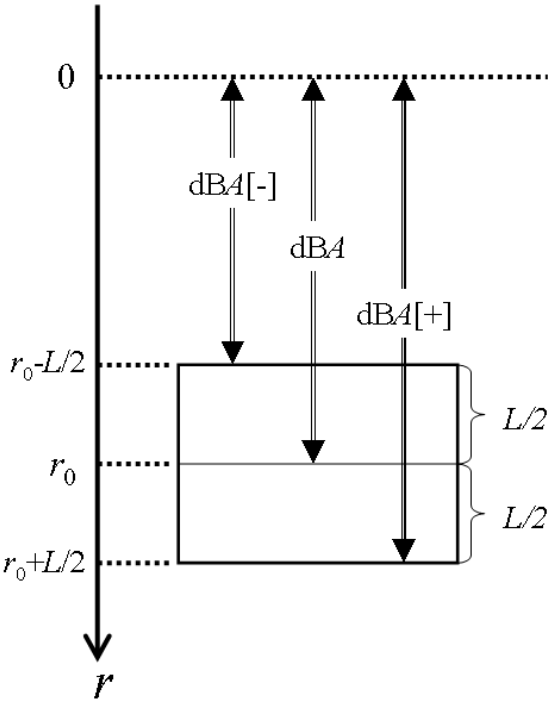

Fig. 2 Different definitions of attenuation for a discrete range.

$$\mathrm{dB}Z_m=\mathrm{dB}Z_e-\mathrm{dB}A[+]. \qquad (16)$$

Please confirm that the following Eq. (17) is hold.

$$\mathrm{dB}A[-]+kL=\mathrm{dB}A=\mathrm{dB}A[+]-kL \qquad (17)$$

For the discussion later in this paper, we define a pseudo observation variable dBZ_e[-2] as Eq. (18).

$$\mathrm{dB}Z_e[-2]\equiv\mathrm{dB}Z_e-2\times kL=\mathrm{dB}Z_m+\mathrm{dB}A[-] \qquad (18)$$

Generally, dB$Z_e[\alpha]$ is defined as Eq. (19).

$$\mathrm{dB}Z_e[\alpha]\equiv\mathrm{dB}Z_e+\alpha\times kL \qquad (19)$$

dB$Z_e[\alpha]$ at a range, for any value of α, is independent of the other ranges as dBZ_e (=dBZ_e[0]) is.

2.4. Primitive problem

The primitive problem in this study is to retrieve (N_0, D_0) of n ranges from dBZ_m of n ranges at the two frequencies of the DPR. This is a set of 2n non-linear equations with 2n unknowns. As shown

in section 2a, ideal conditions can be assumed. Moreover, dBZ_m is assumed to be free from observation errors. SRT can be used to give estimates PIA, but the accuracy of PIA is not guaranteed.

3. RETRIEVAL METHODS

3.1. Forward method (FM)

In forward method (FM), DSD parameters are sequentially determined from near range (range 1) to far range (range *n*) without the use of SRT. At range 1, dBA[-] is assumed to be zero (as no attenuation occurs over the top of precipitation) and dBZ_m is observed, so according to Eq. (18) dBZ_e[-2] is calculated at the two frequencies. Here, we have a smaller problem or a lemma to retrieve (N_0, D_0) from dBZ_e[-2] at the two frequencies. This lemma is just a set of 2 non-linear equations with 2 unknowns, and is indicated by Lemma[-2]. Generally, a lemma to retrieve (N_0, D_0) from $dBZ_e[\alpha]$ of the two frequencies is indicated by Lemma[α]. When the Lemma[-2] is solved at range 1, all the variables at range 1 become known; dBA[+] can be calculated as $dBA[-]+2kL$. As dBA[-] at range 2 is known to be equal to dBA[+] at range 1, the same process can be applied to range 2 after range 1. By repeating this process up to range *n*, (N_0, D_0) and other variables of *n* ranges can be retrieved.

3.2. Backward method (BM)

In backward method (BM), DSD parameters are sequentially determined from far range (range *n*) to near range (range 1) with the use of SRT. At range *n*, dBA[+] is no other than PIA, which can be estimated by SRT, and that dBZ_m is observed, then dBZ_e can be easily calculated according to Eq. (16). Here, we have a lemma to retrieve (N_0, D_0) from dBZ_e at the two frequencies. As dBZ_e is same as dBZ_e[0], the lemma can be indicated by Lemma[0]. When the Lemma[0] is solved at range *n*, all the variables at range n become known; dBA[-] can be calculated as $dBA[+]-2kL$. As dBA[+] at range (*n*-1) is known to be equal to dBA[-] at range *n*, the same process can be applied to range (*n*-1) after range n. By repeating this process up to range 1, (N_0, D_0) and other related variables of *n* ranges can be obtained. BM is essentially same with the retrieval method in ME92.

3.3. Iterative backward method (IBM)

In iterative backward method (IBM), the same procedure with BM is applied without SRT. At first, PIA is assumed arbitrarily, then (N_0, D_0) are sequentially retrieved from range *n* to range 1 as BM. Once (N_0, D_0) of *n* ranges are retrieved, PIA is calculated from the retrieved (N_0, D_0), and the calculated PIA is compared with the assumed PIA. This comparison is equivalent to check that dBA[-] at range 1 is zero or not. If the calculated PIA and the assumed PIA are not same (dBA[-] at range 1 is not zero), assumed PIA turns out wrong. By using differently assumed PIA, the same procedure is iterated till the calculated PIA and the assumed PIA becomes same. In MA04, PIA is assumed to be zero at the first iteration, then at the second iteration and later, PIA is assumed to be same with the calculated PIA at the previous iteration.

3.4. Comparison of methods

As no attenuation occurs over the top of precipitation, dBA[-] at range 1 should be zero. Hereafter, it is called upper boundary condition. The upper boundary condition is satisfied in FM and IBM, but it is not checked in BM. On the other hand, dBA[+] at range *n* should be equal to the true PIA. It is called lower boundary condition. The lower boundary condition is checked neither in FM nor in IBM. From the view point of the boundary conditions on attenuation, FM and IBM are equivalent, while BM is something different from the other two methods. According to the categorization of retrieval methods for single-frequency radar (Iguchi et al, 1994), FM and IBM are kinds of initial value method, while BM is a kind of final value method.

4. SOLUTIONS OF LEMMAS

Any of the three retrieval methods for DPR consists of Lemma[α] (α=-2 or α=0). Except for solving lemmas, no difficulties are involved in the methods. Therefore, in this section, solutions of the lemmas are investigated. As defined, Lemma[α] is

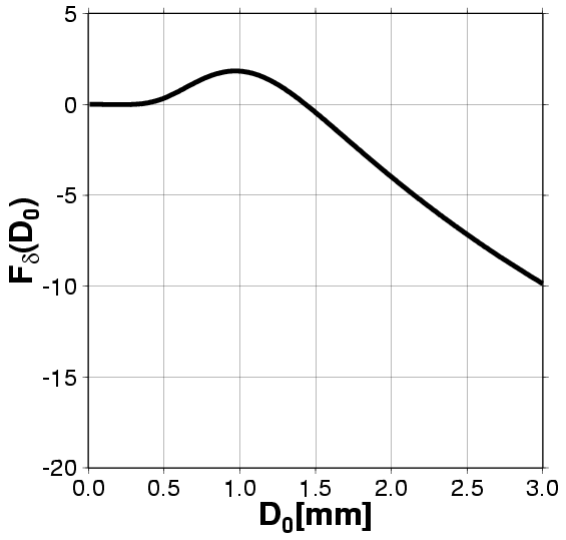

Fig. 3 A function of $F_\delta(D_0)$ in case of T=300 and μ=3.

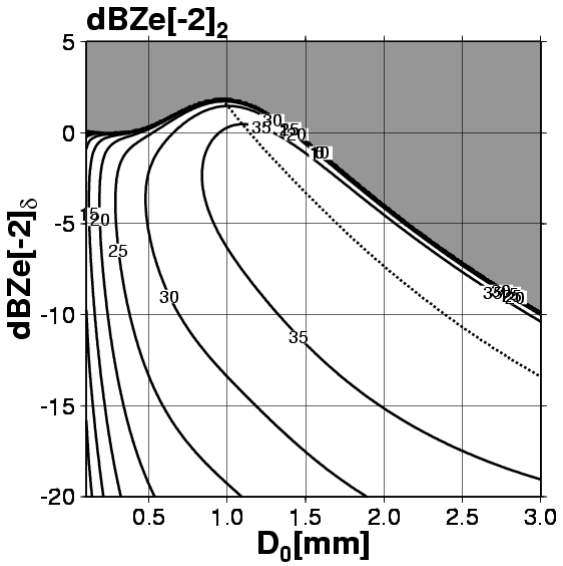

Fig. 4 Contours of dBZ_e[-2]$_2$ in case of T=300 and μ=3. Gray region indicates no solutions are given. Dotted line indicates that ∂ dBZ_e[-2]$_2$/ ∂ D_0=0.

the problem to retrieve (N_0, D_0) from dBZ_e[α] at the two frequencies. dBZ_e[α] can be rewritten as Eq. (20) from Eqs. (10), (11), and (19).

$$\mathrm{dBZe}[\alpha]_i=10\log_{10}(N_0)+F_i(D_0)+\alpha\times N_0\times G_i(D_0)\times L, \quad (20)$$

where subscript i indicates the frequency; 1 is for Ku-band and 2 is for Ka-band. Hereafter, the subscript i can be attached to variables and functions dependent on the frequency.

For α=0, the third term of the right hand side in Eq. (20) is zero, and Eq. (20) can be simplified as follows.

$$\mathrm{dB}Z_e[0]_1=10\log_{10}(N_0)+F_1(D_0), \quad (21\text{-}1)$$

$$\mathrm{dB}Z_e[0]_2=10\log_{10}(N_0)+F_2(D_0). \quad (21\text{-}2)$$

By taking the difference of the two equations in Eq. (21), the first term of the right hand side is cancelled as Eq. (22).

$$\mathrm{dB}Z_e[0]_\delta=F_\delta(D_0), \quad (22)$$

where subscript δ indicates the difference of Ka band and Ku band, or $X_\delta=X_2-X_1$ is hold for any variable X. Eq. (22) has only one unknown parameter D_0. Figure 3 draws the function of $F_\delta(D_0)$ with μ=3.0 and T=300[K]. $F_\delta(D_0)$ takes a local maximum when D_0 is 0.97mm. As far as investigated in our study and also in previous studies, $F_\delta(D_0)$ takes only one local maximum in case of rain drops. D_0 which gives the local maximum of $F_\delta(D_0)$ is indicated by D_{0s}. If dBZ_e[0]$_\delta$ is negative, D_0 is uniquely determined from Eq. (22). However, if dBZ_e[0]$_\delta$ is positive, two different D_0 can satisfy Eq. (22) except for the case of dBZ_e[0]$_\delta$=$F_\delta(D_{0s})$. One of the two D_0 is larger than D_{0s} and another is smaller than D_{0s}, the former of which yields higher rain rates than the latter. In order not to miss heavy rainfall rather weak rainfall, it is a reasonable way to assume that D_0 is larger than or equal to D_{0s}. With this assumption (called D_{0s}-assumption), D_0 is always uniquely determined. When D_0 is determined, by substituting D_0 into Eq. (21-1) or (21-2), N_0 can be calculated. As shown above, Lemma[0] has only one solution under D_{0s}-assumption. Still, when dBZ_e[0]$_\delta$ is given to be larger than $F_\delta(D_{0s})$ because of some errors (such as biases in PIA), no D_0 can satisfy Eq. (22). In such cases, Lemma[0] has no solutions.

Next, Lemma[-2] is considered. dBZ_e[-2] can be written as follows.

$$\mathrm{dB}Z_e[-2]_1=10\log_{10}(N_0)+F_1(D_0)-2\times N_0\times G_1(D_0)\times L, \quad (23\text{-}1)$$

$$\mathrm{dB}Z_e[-2]_2=10\log_{10}(N_0)+F_2(D_0)-2\times N_0\times G_2(D_0)\times L. \quad (23\text{-}2)$$

And, the difference in dBZ_e[-2] between the two frequencies is given as Eq. (24).

$$\mathrm{dB}Z_e[-2]_\delta=F_\delta(D_0)-2\times N_0\times G_\delta(D_0)\times L. \quad (24)$$

Here, the solution of (N_0, D_0) in Lemma[-2] can be visually investigated by Fig. 4, where the horizontal axis is D_0 and the vertical axis is dBZ_e[-2] . When dBZ_e[-2] and D_0 are known, N_0 can be calculated from Eq. (24), and dBZ_e[-2]$_i$ (i=1 or 2) can be calculated by substituting N_0 and D_0 into Eq. (23). In Fig.

4, the contours of $dBZ_e[-2]_2$ are drawn with μ=3 and T=300K. Gray shade indicates the region where a negative N_0 is calculated. On the border line of the gray shade region, N_0=0. We can confirm that the border line is same with the line drawn in Fig. 3.

The solutions of Lemma[-2] correspond to the crossing points of the line for a given $dBZ_e[-2]_\delta$ (parallel to the horizontal axis) and the contour line for a given $dBZ_e[-2]_2$. It is implied by a visual investigation that Lemma[-2] has two solutions and that one solution is located left to the dotted line, which corresponds to $\partial\, dBZ_e[-2]_2 / \partial\, D_0=0$, and another solution is located right to the dotted line. For example, when $dBZ_e[-2]_1$=40dB and $dBZ_e[-2]_2$=35dB ($dBZ_e[-2]_\delta$=-5dB), two solutions are found around D_0=1.4mm and D_0=2.1mm. In this case, the both solutions have D_0 larger than D_{0s}, therefore two solutions coexist even with D_{0s}-assumption. Generally, it can be concluded that the number of solutions of Lemma[-2] is two without D_{0s}-assumption and one or two with D_{0s}-assumption. Exceptionally, Lemma[-2] can have no solutions when biased $dBZ_e[-2]_i$ are given.

5. SOLUTIONS OF PRIMITIVE PROBLEMS: CASE STUDIES

When FM is applied without D_{0s}-assumption, a primitive problem has multiple solutions including the right solution. Even with D_{0s}-assumption, multiple solutions exist for some cases. When BM is applied with D_{0s}-assumption, only one solution is derived, but it is not necessarily the right solution as the PIA estimate may be biased. In this section, BM is applied with PIA estimates of different biases in order to evaluate how biases in PIA affect the estimate of surface rain rate (rain rate at range n; indicated by R_s). From this analysis, we can also see the limitations of IBM and FM.

For the above purposes, simple rainfall cases are tested. In all the cases, DSD parameters (N_0, D_0, μ) and T are set to be constant over n ranges for simplicity though it is not physically realistic particularly for T. μ=3 and T=300K and they are known parameters. (N_0, D_0) are unknown and the retrieval methods do not assume that the parameters are constant over n ranges. PIA estimates have biases of between -5 dB and 5 dB independently of the frequencies. D_{0s}-assumption is employed. When PIA is biased, $dBZ_e[0]$ may become larger than $F_\delta(D_{0s})$. In such case, any D_0 can not satisfy Eq. (22) and the retrieval has to be terminated. When DSD parameters are retrieved up to range 1, $dBA[-]_i$ at range 1 (hereafter, simply denoted by $dBA[-]_i$) is calculated. As is explained, the upper boundary condition that both $dBA[-]_1$ and $dBA[-]_2$ are zero is generally not satisfied in BM.

In Fig. 5, the horizontal axis is for the bias of PIA at Ku-band (indicated by ΔPIA_1) and the vertical axis is for the bias of PIA at Ka-band (indicated by ΔPIA_2). The lower boundary condition is satisfied at the origin (indicated by O; ΔPIA_1=0 and ΔPIA_2=0). Solid line indicates that $dBA[-]_1$=0 and dotted line indicates that $dBA[-]_2$=0. The upper boundary condition is satisfied at the crossing points of the two lines.

5.1. Necessity of SRT

In case 1, N_0=10000, D_0=1.5mm, and n=10. Rain rate is as weak as about 2.1 mm h^{-1}. Fig. 5a is shown for this case, where it should be noted that no lines are drawn as the retrieval is terminated in the left upper part. The upper boundary condition is satisfied only at O, where the lower boundary condition is satisfied. In this case, the upper boundary condition and the lower boundary condition are equivalent, and it is implied that IBM can give the right solution for this case.

In case 2, N_0=10000, D_0=2.0mm, and n=10. Rain rate is about 19.1 mm h^{-1} and is much heavier than case 1. In Fig. 5b, the dotted line is almost overlapped with the solid line while the dotted contour line is also drawn in the right part of this figure. It means that the upper boundary condition is almost or exactly satisfied not only at O. In other words, in some cases that PIA is assumed wrongly (the lower boundary condition is not satisfied), the upper boundary condition is almost or exactly satisfied. For such cases, it can not be expected that IBM gives the right solution.

To investigate the reason of the difference between case 1 and case 2, supplemental cases with smaller n are tested. Case 1-1 is same with case 1, but n=1. As the two lines are overlapped only at the origin (Fig. 5c), it is suggested that IBM

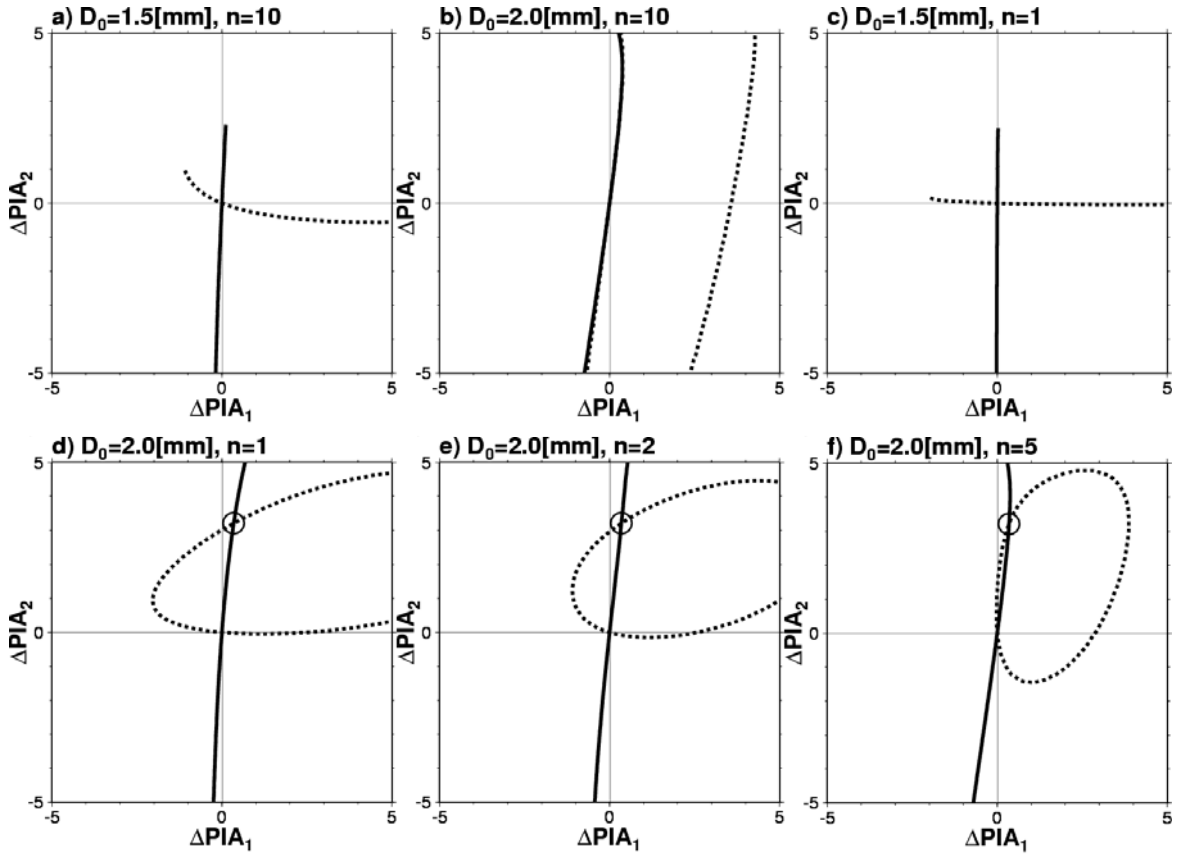

Fig. 5 Figures to check if the upper boundary condition is satisfied or not. On the solid (dotted) line, the upper boundary condition at Ku-band (Ka-band) is satisfied. a) is for case 1, b) is for case 2, c) is for case 1-1, d) is for case 2-1, e) is for case 2-2, and f) is for case 2-5. In b), part of dotted line is overlapped with solid line. In d) to f), an open circle indicates the point A.

can give the right solution. When FM is applied for this case, Lemma[-2] has two solutions; (N_0, D_0)=(10000, 1.5) and (82082120, 0.626). As the latter (wrong) solution has D_0 smaller than D_{0s}, it is not satisfied with D_{0s}-assumption. Therefore, FM as well as IBM has only one solution for case 1-1. For cases with any n (DSD parameters are same as case 1) including case 1 itself, FM should have only one solution. Moreover, considering the equivalence between FM and IBM, it is suggested that IBM has only one solution for such cases.

Case 2-1 is same with case 2, but n=1. As shown in Fig. 5d, the upper boundary condition is satisfied at two points: O and another point (indicated by A). It means that IBM has two solutions (indicated by the solution O and the solution A). When FM is applied for this case, Lemma[-2] has two solutions; (N_0, D_0)=(10000, 2.0) and (125862, 1.596). The former corresponds to the solution O and the latter corresponds to the solution A. As D_0 of the solution A is larger than D_{0s}, the solution A is not rejected by D_{0s}-assumption. As a result, FM as well as IBM has 2 solutions for case 2-1.

Case 2-2 is same with case 2, but n=2. In Fig. 5e, the upper boundary condition is satisfied at two points O and A. The point A in Fig. 5e is exactly same as the point A in Fig. 5d. When FM is applied for this case, Lemma[-2] at range 1 is same as of the case 2-1. If the right solution is selected at range 1, Lemma[-2] at range 2 is also same as of the case 2-1. The right solution is obtained when the selection is right at the two ranges. If the selection is right at range 1 but wrong at range 2, the calculated PIA is biased to the point A. If the selection is wrong at range 1, as dBA[+] at range 1 (=dBA[-] at range 2) is wrongly estimated, Lemma[-2] at range 2 becomes something different from that at range 1. In this case, as dBZ_e[-2]i are biased, this Lemma[-2]

at range 2 has no solutions.

It can be said that FM has only two solutions O and A for any n larger than 1 (DSD parameters are same as case 2). Generally, the solution A can be defined that the right solution is selected at ranges 1 through (n-1) but the wrong solution is selected at range n (as conceptually shown in Fig. 6). If the wrong solution is selected at any range up to (n-1), Lemma[-2] at the next range has no solutions. Accordingly, this primitive problem can not have other solutions than O and A in case 2 (n=10). Considering the equivalence of FM and IBM, IBM should have only two solutions in case 2. Although it is difficult to see in Fig. 5b if the two contour lines overlap with each other exactly or not, it is now clear that the two contour lines cross only at the two points O and A. Still, along the straight line linking O and A, the upper boundary condition is almost satisfied. If any PIA on the straight line OA is assumed in IBM, as the upper boundary condition is almost satisfied, the biased PIA can be judged to be right unless numerical calculation is done with very high precision.

Here, we acknowledge that IBM has two kinds of solutions; they can be called “exact solutions” and “approximate solutions”. The exact solutions satisfy the upper boundary condition exactly and the approximate solutions satisfy the upper boundary condition with small error which is difficult to be detected in practical numerical calculation. The approximate solutions become apparent as n increases. Fig. 5f is for the case same with case 2 but n=5. The two contour lines are close to each other compared with case 2-1 (n=1) and case 2-2 (n=2), still can be distinguished differently from case 2 (n=10). When multiple solutions exist, IBM can not select the right solution objectively. In such cases, PIA estimates by SRT are required to distinguish the right solution from other exact and approximate solutions.

5.2. Required accuracy of PIA

The relative error in surface rain rate derived by BM with biased PIA estimates for case 2 is shown in Fig. 7. The relative error is calculated as $[R_s\text{-}R_s(O)]/R_s(O)$, where $R_s(O)$ is surface rain rate of the right solution. When PIA_2 is biased, larger error in R_s is generated than when PIA_1 is biased to the

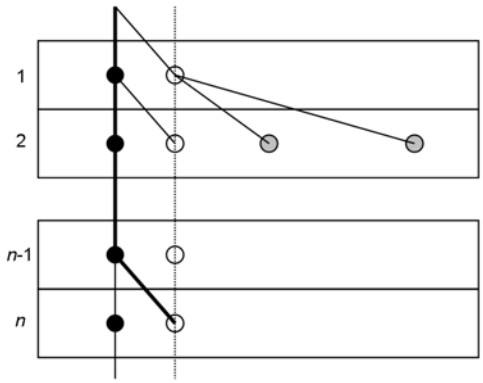

Fig. 6 A schematic figure of multiple solutions for primitive problem. Horizontal direction corresponds to the bias in attenuation. Closed circles indicate the right solution and open circles indicate the wrong solution at each range. The profile of solution A is shown by thick solid lines. At range 2, there may exist other two solutions as shown by gray circles, but not in case 2.

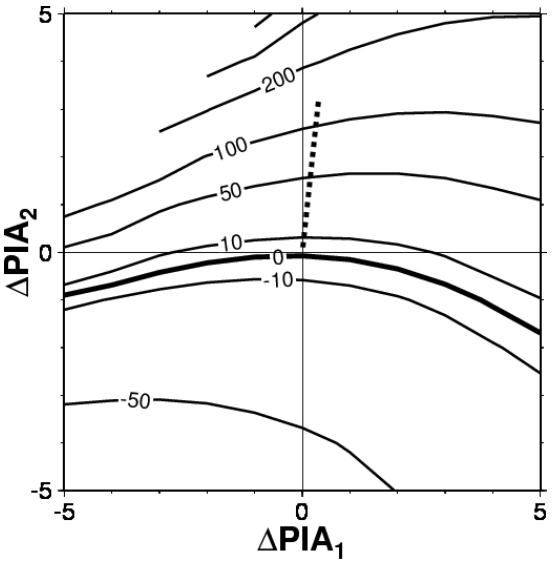

Fig. 7 The relative error in R_s derived by BM with biased PIA for case 2. Dotted line shows the straight line linking the points O and A, where candidates of solutions are assumed to exist.

same extent.

In IBM, by checking the upper boundary condition, (ΔPIA_1, ΔPIA_2) is constrained. It can be assumed in case 2 that candidates of solutions exist on the straight line linking the points O and A. Therefore, to select unique solution, PIA estimates at both frequencies are not necessary. If a PIA estimate at either frequency is given by SRT, by combining this estimate with IBM, unique solution can be obtained. This is a modified IBM. Instead of a PIA estimate at single frequency, the difference of PIA estimates at dual frequencies ($PIA_\delta \equiv PIA_2$-PIA_1) can be used. As was explained in section 1, PIA estimates are subject to biases caused by the change of land surface conditions. It is expected that PIA_δ has smaller biases than PIA_1 and PIA_2 as biases in PIA_1 and PIA_2 are partly cancelled, though it has not been supported yet by observations. This modified IBM is similar to a method proposed in Adhikari et al. (2007), which used DA instead of PIA_δ.

Approximate solutions with relative error in R_s of 10% (50%) are called solution B (C). For case 2, (ΔPIA_1, ΔPIA_2) is (0.045dB, 0.418dB) for solution B and (0.138dB, 1.697dB) for solution C. Required accuracy in PIA at Ku-band is much higher than that at Ka-band. It seems very difficult to satisfy the required accuracy at Ku-band from the experience of TRMM/PR. Although the authors have no information on possible accuracy of PIA estimates at Ka-band by SRT, it is assumed to be same as that at Ku-band in the rest of this paper. It may be possible to satisfy the required accuracy at Ka-band if the relative error in R_s of 50% is allowed.

6. SOLUTIONS OF PRIMITIVE PROBLEMS: GENERAL RESULTS

In previous section, solutions of primitive problems are investigated for some cases. In this section, more general cases are investigated to derive robust results.

6.1.The dependence on D_0

Same as the previous section, DSD parameters (N_0, D_0, μ) and T are set to be constant over n ranges. N_0=10000, μ=3, T=300K, and D_0 is different by cases (between 0.5mm and 3.5mm). Learned from the results of the previous section, the solution A is focused. Particularly, (N_0, D_0) at range n, R_s, and ΔPIA_i of the solution A are examined (Fig. 8). Actually, these variables are independent of n, so they can be obtained just by solving the Lemma[-2]. Hereafter, if not explicitly notified, (N_0, D_0) indicates values at range n. An estimate of the solution X is indicated by putting (X) to the variable. For example, D_0(A) indicates the D_0 at range n of the solution A.

1) Categorization

Here, the primitive problem can be categorized into several types by D_0(O). When D_0(O) is smaller than D_{0s}(=0.97mm), the right solution can not be selected as we assume that D_0 should be larger or equal to D_{0s}. In this case, the primitive problem is categorized as type-0 and is excluded from this study.

When D_0(O) becomes larger than D_{0s}, it holds that D_0(A)<D_0(O), R_s(A)>R_s(O), ΔPIA_1(A)>0, and ΔPIA_2(A)>0. As long as the inequalities hold, the primitive problem is categorized as type-1. The upper limit of D_0(O) in type-1 is indicated by D_{0x}. When D_0(O)=D_{0x}, the solution A becomes identical with the solution O. Here, D_{0x}=2.17mm and the corresponding R_s(O) is 35.4 mm h^{-1}. Type-1 is further divided into type-1a and type-1b by comparing D_0(A) and D_{0s}. When D_0(A) is smaller than D_{0s}, by D_{0s}-assumption, the right solution O is uniquely selected. In this case, the primitive problem is categorized as type-1a. On the other hand, when D_0(A) is larger than D_{0s}, the solution A can not be rejected by D_{0s}-assumption, and the primitive problem is categorized as type-1b. D_0(O) of type-1a is smaller than that of type-1b, and the threshold of D_0(O) between the two types is indicated as D_{0w}. Here, D_{0w} is 1.77mm and the corresponding R_s(O) is 7.57 mm h^{-1}. The case 1 is involved in type-1a and the case 2 is involved in type-1b.

When D_0(O) becomes larger than D_{0x}, it holds that D_0(A)>D_0(O), R_s(A)<R_s(O), ΔPIA_1(A)<0, and ΔPIA_2(A)<0. The upper limit of D_0(O) to satisfy the inequalities is indicated by D_{0y}. When D_0(O) approaches to D_{0y}, D_0(A) diverges to positive infinity. D_{0y} is estimated to be around 2.67mm and the corresponding R_s(O) is about 167 mm h^{-1}. When D_0(O)

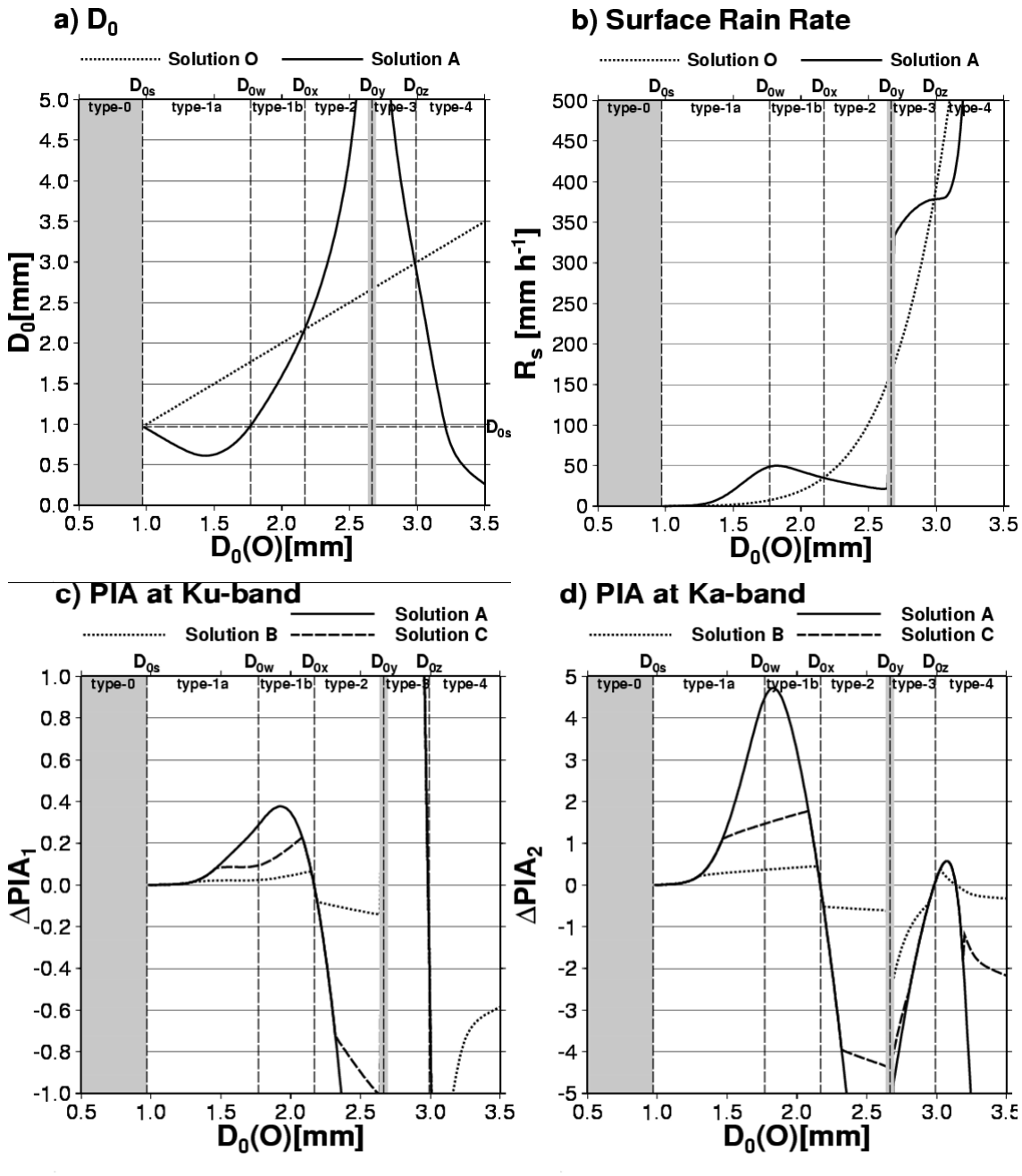

Fig. 8 Categorization of the primitive problem with different D_0(O). a) D_0, b) surface rain rate, c) PIA at Ku-band, and d) PIA at Ka-band of the right and wrong solutions are shown.

is between D_{0x} and D_{0y}, the primitive problem is categorized as type-2.

More two types are defined for D_0(O) larger than D_{0y}. When D_0(O) exceeds to D_{0y}, D_0(A) starts to decrease and it holds that D_0(A)>D_0(O), R_s(A)>R_s(O), ΔPIA_1(A)>0, and ΔPIA_2(A)<0. In these cases, the primitive problem is categorized as type-3. The upper limit of D_0(O) in type-3 is indicated by D_{0z}. Here, D_{0z} is 2.99mm and the corresponding R_s(O) is 385 mm h^{-1}. When D_0(O) is equal to D_{0z}, the solution A becomes identical with the solution O. When D_0(O) is larger than D_{0z}, the primitive problem is categorized as type-4. In type-4, D_0(A) is smaller than D_0(O) and PIA_1(A) is

smaller than PIA_1(O), but the order of R_s(A) and R_s(O) and that of PIA_2(A) and PIA_2(O) are not fixed. It might not be very important to consider type 3 and type 4 because rain echoes at near surface are masked under extremely heavy rainfall.

2) The role of SRT

The role of SRT is examined for each type. Approximate solutions B and C are defined as in section 5, but if the relative error in R_s(A) is negative, approximate solutions with relative error in R_s of -10% (-50%) are called solution B (C). If the relative error in R_s(A) is within 10%, the solutions B and C are not defined. If the relative error in R_s(A) is within 50%, the solution C is not defined. In Fig. 8c and 8d, ΔPIA_1 and ΔPIA_2 of the solutions B and C are shown as well as those of the solution A.

While SRT is not necessary for type-1a as the solution A is rejected by D_{0s}-assumption, SRT is necessary for the other types. In type-1b, both ΔPIA_1(A) and ΔPIA_2(A) are positive and that ΔPIA_2(A) is nearly ten times as large as ΔPIA_1(A). Therefore, it is much effective to estimate PIA by SRT at Ka-band rather than at Ku-band for the modified IBM. ΔPIA1(A) and ΔPIA_2(A) become zero when D_0(O) approaches to D_{0s} or D_{0x}. It becomes more difficult but less necessary to distinguish O and A, as the difference in R_s between O and A becomes small. In type 1b, as ΔPIA_1(B) is smaller than 0.1dB and ΔPIA_2(B) is smaller than 0.5dB, it seems to be difficult to distinguish O from B unless SRT would be significantly improved compared with the TRMM era. On the other hand, it can be expected to distinguish O from C as ΔPIA_2(C) is larger than 1dB, while ΔPIA_1(C) is smaller than 0.2dB.

Required accuracy in PIA_δ is slightly higher than PIA_2. Still, if biases in PIA_i are effectively cancelled by taking the difference, using PIA_δ leads to better estimates in R_s than using PIA2.

In type 2, both ΔPIA_1(A) and ΔPIA_2(A) are negative and that $|\Delta PIA_2|$ is nearly ten times as large as $|\Delta PIA_1|$. Same as type 1, it is much effective to estimate PIA at Ka-band than at Ku-band. When D_0(O) increases, ΔPIA_1(A) and ΔPIA_2(A) increase rapidly, therefore it is not difficult to distinguish O from A. There is some possibility to distinguish O from B by means of SRT at Ka-band as ΔPIA_2(B) is larger than 0.5dB, while ΔPIA_1(B) is around 0.1dB. Moreover, as ΔPIA_1(C) is near to 1dB and ΔPIA_2(C) is larger than 4dB, it can be expected to distinguish O from C by SRT at Ku-band as well as by SRT at Ka-band.

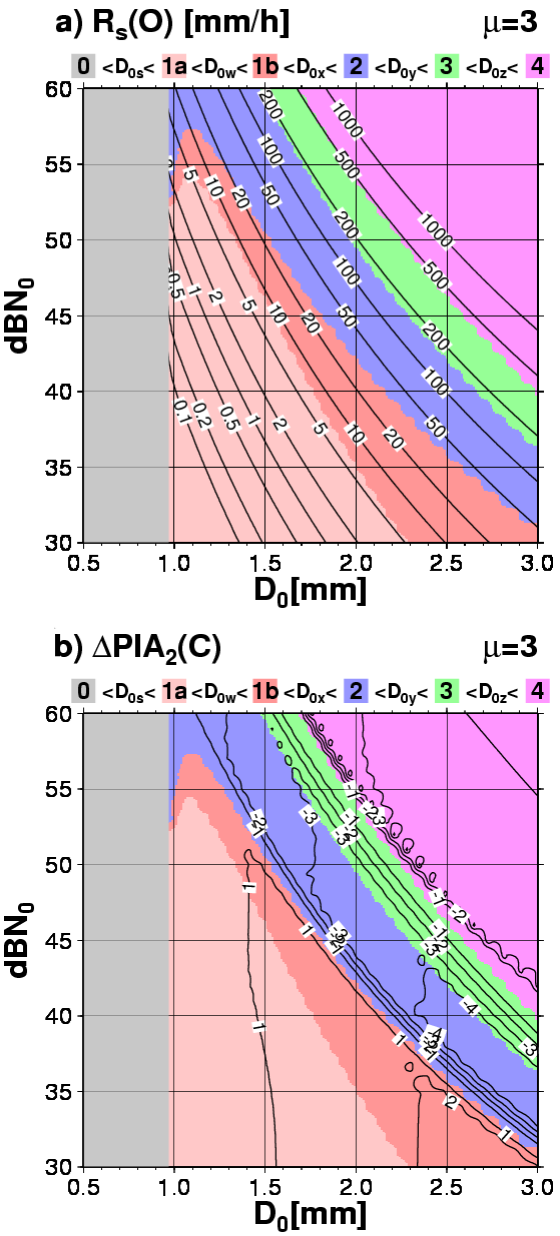

Fig. 9 Categorization of the primitive problem is shown by different background colors (gray for type-0, light pink for type-1a, dark pink for type-1b, blue for type-2, green for type-3, and purple for type-4). a) R_s(O) and b) ΔPIA_2(C) are shown as contours. μ is set to be 3.

In type 3 and in part of type 4, $\Delta PIA_1(A)$ and $\Delta PIA_2(A)$ have different signs and $|\Delta PIA_1(A)|$ is generally larger than $|\Delta PIA_2(A)|$. It is more effective to use PIA at Ku-band rather than at Ka-band. If PIA at both frequencies are available, using PIA_δ may gives better accuracy.

6.2.The dependence on N_0

The same simulation with the previous subsection 6a is done but for different N_0 ranging from 1,000 (dBN_0=30dB) to 1,000,000 (dBN_0=60dB) with the step of 1dB, where dBN_0 indicates $10\log_{10}N_0$.

In Fig. 9a, different types are shown by different background colors on the plane of (D_0, dBN_0) with the contour of R_s(O). Note that D_{0s} is independent of N_0 as it is determined by Eq. (22). D_{0w}, D_{0x}, D_{0y}, and D_{0z} are dependent on N_0, and they tend to become small as N_0 becomes large. When N_0 is larger than 54dB, type-1a does not exist. Furthermore, when N_0 is larger than 57dB, type-1b is not found. Except for these high N_0 cases, R_s(O) at the border of different types are not very sensitive to N_0. The upper limit of R_s(O) in type-1a is 5 to 10 mm h^{-1}, that in type-1b is around 20 to 50 mm h^{-1}, that in type-2 is around 150 to 200 mm h^{-1}, and that in type-3 is nearly 500 mm h^{-1}. Roughly speaking, SRT is not necessary when R_s(O) is lower than 5 mm h^{-1}, on the other hand, SRT is required when R_s(O) is higher than 10 mm h^{-1}.

The contour of $\Delta PIA_2(C)$ is shown in Fig. 9b. When D_0(O) is close to D_{0x} or D_{0z}, as the solution C does not exist, $\Delta PIA_2(A)$ is shown instead of $\Delta PIA_2(C)$. In type 1b, $|\Delta PIA_2(C)|$ is generally larger than 1dB where N_0 is smaller than 50dB. In type 2, except for the case that D_0(O) is close to D_{0x}, $|\Delta PIA_2(C)|$ is larger than 1dB and exceeds to 4dB when N_0 is smaller.

6.3.The dependence on μ

Up to here, the third DSD parameter μ is fixed to be 3, but the results may be significantly changed by different μ. In this subsection, μ is fixed to be 1, and the same simulation with subsection 6b is done (Fig. 10). D_{0s} for μ=1 is 0.71mm and smaller than that for μ=3. Other thresholds of D_0(O)

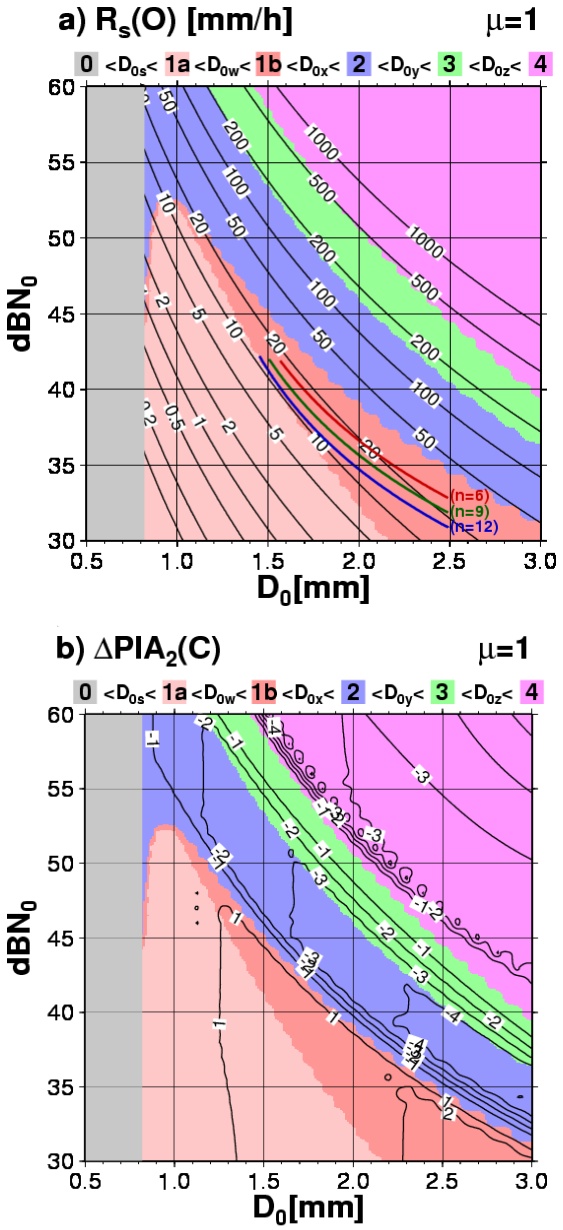

Fig. 10 Same as Fig. 9, but for μ=1. In a), the threshold below which MA04's method can give the right solution is shown according to RC05.

are also smaller for μ=1 than those for μ=3. However, the upper limit of R_s(O) in each type is nearly same with the case of μ=3. Moreover, the contour of $\Delta PIA_2(C)$ for μ=1 shown in Fig. 10b is basically similar to that for μ=3 in Fig. 9b. It means that required accuracy of SRT at Ka-band is not very sensitive to μ.

Rose and Chandrasekar (2005) tested

MA04's method (a kind of IBM) for many cases with μ=1, and empirically determined the conditions that MA04's method could give the right solution. If D_0 is smaller than D_0* given in the Eq. (25) [as Eq. (41) of their paper], the right solution is selected by MA04's method.

$$D_0^* = \left(a + \frac{b}{N_w^{0.5}} \right)^2 , \qquad (25)$$

where N_w is normalized intercept parameter of gamma distribution, and can be related with D_0, N_0, and μ by Eq. (26).

$$N_w = N_0 D_0^{\mu} \frac{3.67^4}{6} \frac{\Gamma(\mu+4)}{(3.67+\mu)^{\mu+4}} . \qquad (26)$$

Two variables of Eq. (25) *a* and *b* were empirically determined and were dependent on *n*. The lines corresponding to Eq. (25) are drawn in Fig. 10a for the cases of *n*=6, 9, and 12. As values of *a* and *b* were derived under the conditions that N_w is not larger than 8000 and D_0 is not larger than 2.5mm, the lines in Fig. 10a are drawn within in this limit. It is seen that the three lines are drawn in the region of type 1b. As MA04's method tends to select the solution with the smallest PIA among multiple candidates of solutions, it generally selects the solution O rather than the solution A for type-1b. As it becomes difficult to distinguish O from approximate solutions when *n* increases, it is convincing that the lines shift to weaker R_s(O) when n increases.

Adhikari et al. (2007) also tested MA04's method and showed (N_0, D_0)=(8000, 1.1) as a successful case and (N_0, D_0)=(8000, 1.5) as a failure case. In their study, it was set that μ=0 and *n*=17. We confirmed that the former case belongs to type-1a and the latter case belongs to type-1b by drawing the same figure with Fig. 10a but for μ=0 (not shown). The previous studies found the limitation of MA04's method in the region of type 1b.

6.4.The dependence on the discrete from of dBZ$_m$

As explained in Section 2c, dBZ_m at a discrete range is defined in Eq. (16) up to here in this paper. However in this subsection, the attenuation

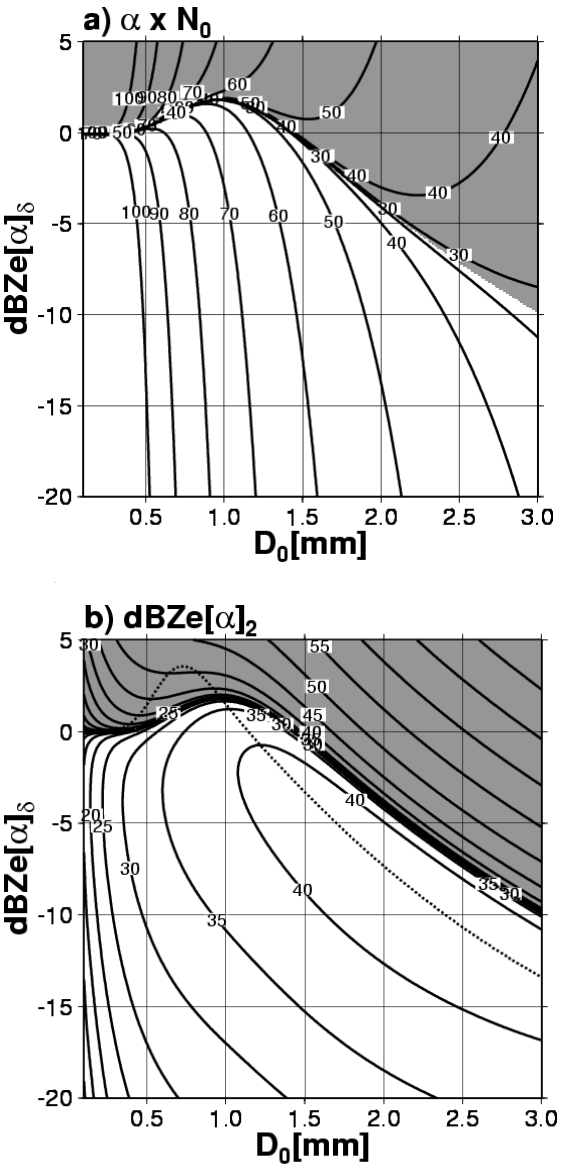

Fig. 11 Figures to visually examine the solutions of Lemma[α]. a) $\alpha \times N_0$ when dBZ_e[α] and D_0 are given. Shaded area indicates $\alpha \times N_0$>0 and plain area indicates $\alpha \times N_0$<0. Contours are drawn for dB|$\alpha \times N_0$|. b) Contours of dBZ_e[α]$_2$. Dotted line indicates that ∂ dBZ_e[α]$_2$/ ∂ D_0=0. α=1 for shaded area and α=-1 for plain area.

is set as dB*A* as shown in Eq. (27), to check if different definitions of dBZ_m affect the conclusions of this paper.

$$dBZ_m = dBZ_e - dBA. \qquad (27)$$

With this definition, the second equality of Eq. (18) does not hold. Instead of that, the following two equations hold.

$$dBZ_m + dBA[-] = dBZ_e - 1 \times k \times L \equiv dBZ_e[-1], \quad (28\text{-}1)$$

$$dBZ_m + dBA[+] = dBZ_e + 1 \times k \times L \equiv dBZ_e[1]. \quad (28\text{-}2)$$

In FM, $dBZ_e[-1]$ is given instead of $dBZ_e[-2]$, then a Lemma[-1] has to be solved at each range. In BM (and IBM), $dBZ_e[1]$ is given instead of $dBZ_e[0]$, then a Lemma[1] has to be solved at each range.

The characteristics of Lemma[-1] and Lemma[1] are explained in a general way as below. Following Eq. (29) can be derived from Eqs. (10), (11), and (19) for any .

$$dBZ_e[\alpha]_\delta = F_\delta(D_0) + \alpha \times N_0 \times G_\delta(D_0) \times L \quad (29)$$

When $dBZ_e[\alpha]$ and D_0 are given, $\alpha \times N_0$ can be calculated. In Fig. 11a, where the horizontal axis is D_0 and the vertical axis is $dBZ_e[\alpha]_\delta$, gray shaded area indicates that $\alpha \times N_0 > 0$ and plain area indicates that $\alpha \times N_0 < 0$. Contours are drawn for $dB|\alpha \times N_0|$. As N_0 should be positive, solutions of Lemma[α] can exist only in gray shaded area when $\alpha > 0$ and only in plain area when $\alpha < 0$. It can be seen that the boundary of shaded area and plain area ($\alpha \times N0 = 0$) is identical with the line in Fig. 3. If α=-2 is applied for plain area, $dBZ_e[-2]_2$ can be calculated as shown in Fig. 4. Same as this, α=-1 is applied for plain area and $dBZ_e[-1]_2$ is calculated. On the other hand, α=1 is applied for shaded area and $dBZ_e[1]_2$ is calculated. In Fig. 11b, $dBZ_e[-1]_2$ and $dBZ_e[1]_2$ are shown together. The dotted line indicates $\partial dBZ_e[\alpha]_2 / \partial D_0 = 0$ (α=-1 for plain area and α=1 for gray shaded area). From a visual investigation, the followings are strongly suggested. Lemma[-1] has two solutions, and at least one of them has D_0 larger than D_{0s}. It is not always possible to get unique solution even with D_{0s}-assumption. Lemma[1] has unique solution when $dBZ_e[1]$ is negative and it has three solutions in some cases when $dBZ_e[1]$ is positive. In the latter case, two of the three solutions have D_0 smaller than D_{0s}. Therefore, it is always possible to get unique solution of Lemma[1] with D_{0s}-assumption. In addition to the above, it should be kept in mind that the lemmas have no solutions in some cases that biased $dBZ_e[\alpha]_i$ are given.

Figure 12 is same as Fig. 9 but with the definition of Eq. (27). D_0(O) at the boundary of

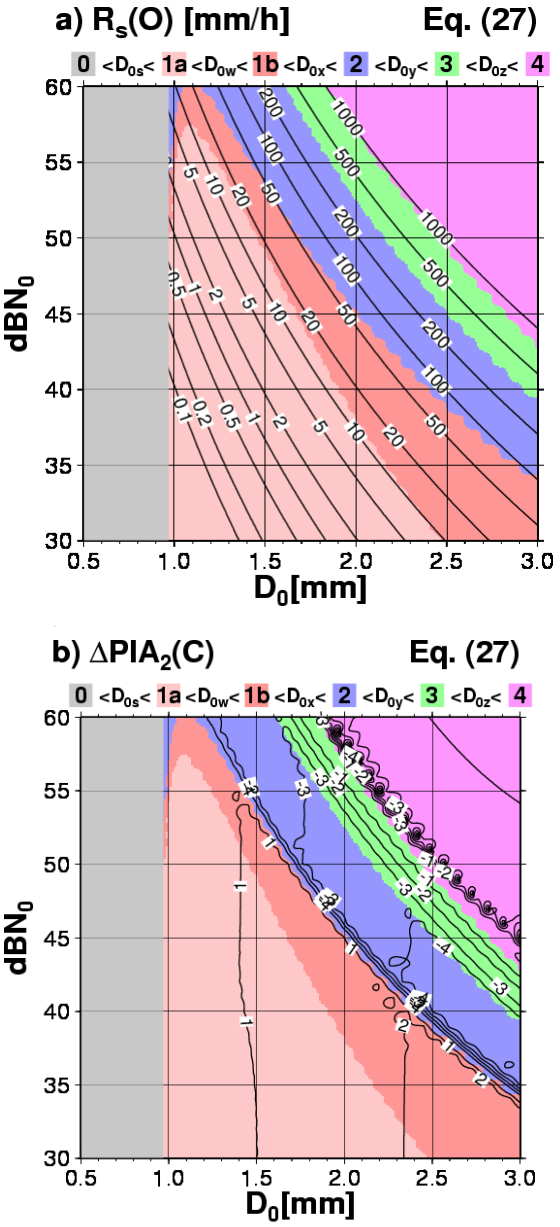

Fig. 12 Same as Fig. 9, but the Eq. (27) is used to define the attenuation at a discrete range in stead of Eq. (16).

different types is slightly larger in Fig. 12a than in Fig. 9a. Corresponding R_s(O) is also slightly larger in Fig. 12a than in Fig. 9a. ΔPIA_2(C) as shown in Fig. 12b is nearly same with that in Fig. 9b. It can be concluded that the main results of this study are not significantly changed by different definitions of dBZ_m.

7. SUMMARY AND CONCLUSIONS

A primitive problem for the GPM/DPR, which derives DSD parameters from observed Z_m, is investigated in this study. This can be treated as a mathematical problem to estimate 2n unknowns from 2n equations. Retrieval methods of this problem such as FM, BM, and IBM, can be decomposed into lemmas to estimate 2 unknowns from 2 equations. Lemmas involved in FM generally have two solutions, so FM yields multiple solutions for the primitive problem. On the other hand, lemmas in BM have unique solution under D_{0s}-assumption, therefore BM can yield the right solution if the PIA is accurately estimated by SRT.

IBM is equivalent to FM as the upper boundary condition is checked but the lower boundary condition is not checked in both methods. There are two types of solutions in IBM: exact solutions and approximate solutions. Exact solutions satisfy the upper boundary condition exactly and they are equivalent to solutions derived in FM. Approximate solutions almost satisfy the upper boundary condition. When n increases, as the numerical error is accumulated, approximate solutions become apparent.

The primitive algorithm is categorized into several types. In type-1a, as the right solution can be selected by D_{0s}-assumption, IBM can yield the right solution. In type-1b, as the solution A can not be objectively rejected, IBM can not be expected to always yield the right solution. However, in MA04's method (a kind of IBM), which tends to select the solution with the smallest PIA, the right solution is selected when rain rate is relatively weak. The upper limit of R_s(O) in type-1b is generally less than 50 mm h^{-1} (though it is dependent on N_0 and μ), but the upper limit of R_s(O) when the right solution can be derived in MA04's method is much smaller because of approximate solutions.

SRT is necessary to solve the primitive problem except for some weak rainfall cases. By combining with IBM, PIA estimate by SRT at either frequency gives unique solution. In type 1b and type 2, required accuracy of PIA estimate by SRT is much higher at Ku-band than at Ka-band. So, it is much effective to estimate PIA at Ka-band if the accuracy of SRT is same at both frequencies. To estimate R_s with a relative error of 50% or better, the required accuracy of PIA estimates at Ka-band is around 1dB in type 1b and around 4dB in type 2. The above results are not strongly dependent on N_0, μ, and the definition of dBZ_m in discrete form.

Though some part of this paper is not mathematically rigorous (such that the number of solutions is judged by a visual investigation), the results are believed to be right for most cases. It is necessary to note that this study assumes many ideal conditions (such that no observation errors in Z_m). To compensate such errors, higher accuracy should be required for SRT. On the other hand, this study does not assume that the relationship between ranges. As Rose and Chandrasekar (2006) assumes that DSD parameters are expressed by linear function of altitude, additional constraint may relax the requirement for SRT.

Acknowledgements. This study is a part of results of a collaborative research "Development of surface reference technique for dual-frequency precipitation radar (PI: S. Seto)" between the Japan Aerospace Exploration Agency (JAXA) and the University of Tokyo.

REFERENCES

Adhikari, N. B., T. Iguchi, S. Seto, and N. Takahashi, 2007: Rain retrieval performance of a dual-frequency precipitation radar technique with differential-attenuation constraint. *IEEE Trans. Geosci. Remote Sens.*, **45**, 2612-2618.

Gunn, R., and G. G. Kinzer, 1949: The terminal velocity of fall for water droplets in stagnant air. *J. Meteorol.*, **6**, 243-248.

Iguchi, T., T. Kozu, J. Kwiatkowski, R. Meneghini, J. Awaka, and K. Okamoto, 2009: Uncertainties in the rain profiling algorithm for the TRMM precipitation radar. *J. Met. Soc. Japan*, **87**(A), 1-30.

Kozu, T., K. Nakamura, R. Meneghini, W. C. Boncyk, 1991: Dual-parameter radar rainfall measuremetn from space: A test result from an aircraft experiment. *IEEE Trans. Geosci. Remote Sens.*, **29**, 690-703.

Liao, L., and R. Meneghini, 2005: A study of

air/space-borne dual-wavelength radar for estimates of rain profiles. *Adv. Atmos. Sci.*, **22**, 841-851.

Mardiana, R., T. Iguchi, and N. Takahashi, 2004: A dual-frequency rain profiling method without the use of a surface reference technique. *IEEE Trans. Geosci. Remote Sens.*, **42**, 2214-2225.

Meneghini, R., T. Kozu, H. Kumagai, and W. C. Boncyk, 1992: A study of rain estimation methods from space using dual-wavelength radar measurments at near-nadir incidence over ocean. *J. Atmos. Oceanic Technol.*, **9**, 364-382.

Seto, S., and T. Iguchi, 2007: Rainfall-induced changes in actual surface backscattering cross sections and effects on rain-rate estimates by spaceborne precipitation radar. *J. Atmos. Oceanic Technol.*, **24**, 1693-1709.

Rose, C. R., and V. Chandrasekar, 2005: A systems approach to GPM dual-frequency retrieval. *IEEE Trans. Geosci. Remote Sens.*, **43**, 1816-1826.

Rose, C. R., and V. Chandrasekar, 2006: A GPM dual-frequency retrieval algorithms: DSD profile-optimization method. *J. Atmos. Oceanic Technol.*, **23**, 1372-1383.